

Supporting Information

Biomass-derived Nickel-based Nanomaterial as a Sustainable and Reusable Catalyst for Hydrogenation of Arenes and Heteroarenes

Vishakha Goyal,^[a, b] Tarun Bhatt,^[c] Anshid Kuttasseri,^[c] Arup Mahata,^{*[c]} Radek Zbořil^{*[a, d]},
Kishore Natte^{*[d]} Rajenahally V. Jagadeesh^{*[a, b]}

[a] Nanotechnology Centre, Centre for Energy and Environmental Technologies, VSB-Technical University of Ostrava, 17. listopadu 2172/15, 708 00, Ostrava Poruba, Czech Republic.

[b] Leibniz-Institut für Katalyse e.V., Albert-Einstein-Straße 29a, 18059 Rostock, Germany.

[c] Department of Chemistry, Indian Institute of Technology, Hyderabad, Kandi, Sangareddy, 502 284, Telangana, India.

[d] Regional Centre of Advanced Technologies and Materials, Czech Advanced Technology and Research Institute (CATRIN), Palacký University Olomouc, Šlechtitelů 27, 77 900 Olomouc, Czech Republic. E-mail:

*Corresponding authors. E-mails: arup@chy.iith.ac.in; radek.zboril@vsb.cz;

kishore.natte@chy.iith.ac.in; jagadeesh.rajenahally@catalysis.de

Table of Contents

1. Materials and methods
2. Characterization data of nickel-based catalysts
3. DFT calculation
4. General procedure for the synthesis of pine needle-derived Ni-catalysts
5. General procedure for the hydrogenation of arenes and heteroarenes
6. General procedure for the recyclability studies
7. Spectral data of products
8. NMR and GCMS spectra

1. Materials and methods

Unless otherwise mentioned, all substrates and reagents were commercially obtained and used without further purification. Pine needles were collected from Tehri Garhwal (Uttarakhand, India). All catalytic reactions were performed in a 25 mL stainless steel autoclave.

Gas chromatography was carried out by Thermo- Scientific Model AI1310 equipped with TG-5MS capillary column (dimension 30m × 0.25mm×0.25µm); carrier gas He, flow rate 1ml/min with the split mode, and the maximum oven temperature 350°C.

NMR spectra were recorded with a Bruker ADVANCE III 500 MHz spectrophotometer using TMS as an internal standard and CDCl₃ as the solvent.

High-resolution transmission electron microscopy (TEM) measurements were performed on a JEM 2100(JEOL, Japan) microscope. The sample was dispersed in the ethanol, followed by ultrasonification to form a suspension solution. One drop of this solution is dropped on the lacey carbon formvar Cu grid.

X-ray photoelectron spectroscopy analysis was carried out using monochromatic Mg Kα radiations. The core carbon 1s was taken as an internal standard (284.6 eV).

X-ray diffraction (XRD) patterns of samples were performed on PROTO AXRD benchtop-ray diffractometer at 40Kv and 30Ma through Niβ filtered Cu Kα radiation ($\lambda=1.5406 \text{ \AA}$) over a 2theta range of 10-80 degree. Textural properties of materials were determined by Micromeritics, ASAP 2020 instrument. Before analysis, the samples were degassed at 250 °C for 5 hours.

Raman Spectra were obtained on Horbia Jobin Yvon Lab Ram HR Evolution Spectrometer equipped with a CCD (charged coupled device) detector using an excitation laser wavelength of 633 nm. H₂-temperature-programmed reduction (TPR) was performed in a quartz tube reactor on Micromeritics, Auto Chem II 2920 equipped with a thermal conductivity detector (TCD).

The surface basicity of the samples was measured by CO₂-TPD (temperature-programmed desorption) technique by using Micromeritics, Auto Chem -11 2920 instrument. The sample (50 mg) was pre-treated at 680°C in the presence of He. Then saturate the sample with CO₂ at 100°C and flush it with He to remove physically adsorbed CO₂. finally, CO₂ desorption was measured with a heating rate of 10 °C/min up to 700 °C in the presence of He.

Magnetic measurements were recorded on the MPMS3 system with High homogeneity magnet configuration: ± 7.0 Tesla, Field Uniformity 0.01% Quantum Design MPMS-XL superconducting quantum interference device (SQUID) magnetometer at different temperatures and applied magnetic field. The sample was dried in a vacuum oven at 120 °C for 12 hours in Labtech, Daihan Labtech Co. Ltd.

The reactions were monitored by thin-layer chromatography (TLC) using silica gel plates (TLC Silica gel 60 F254), and compounds were monitored/visualized with UV light.

Table S1. Effect of solvents

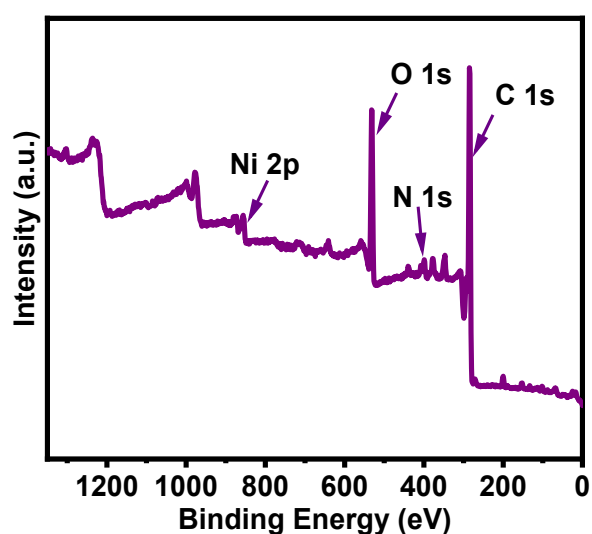
S. No.	Catalyst	Solvent	Conversion (%)	Yield (%)
1	Ni-NPs@NBC-700	toluene	8	3
2	Ni-NPs@NBC-700	n-hexane	6	2
3	Ni-NPs@NBC-700	1,4-dioxane	30	25
4	Ni-NPs@NBC-700	tetrahydrofuran	45	40
5	Ni-NPs@NBC-700	<i>t</i> -butanol	60	55
6	Ni-NPs@NBC-700	ethanol	50	45
7	Ni-NPs@NBC-700	distilled water	92	90
8	Ni-NPs@NBC-700	IPA	>99	99

Reaction Conditions: 0.5 mmol quinoline, 50 mg catalyst, 30 bar H₂, 2 mL isopropanol, 120 °C, and 24 h; conversion and yields were determined by GC using n-hexadecane standard.

2. Characterization data of nickel-based catalysts

Table S2. Elemental analysis of nickel-based catalysts and raw pine needle.

Entry	Catalyst	Ni wt%	N wt%	C wt%	H wt%	S wt%
1	Ni-NPs@NBC-600	9.4	1.34	59.10	1.803	0.321
2	Ni-NPs@NBC-700	9.5	0.94	65.74	1.650	0.176
3	Ni-NPs@NBC-800	9.1	0.83	61.05	1.553	0.358
4	Raw Pine Needle	-	1.52	72.08	2.78	1.976

**Figure S1.** Survey XPS of Ni-NPs@NBC-700 catalyst.

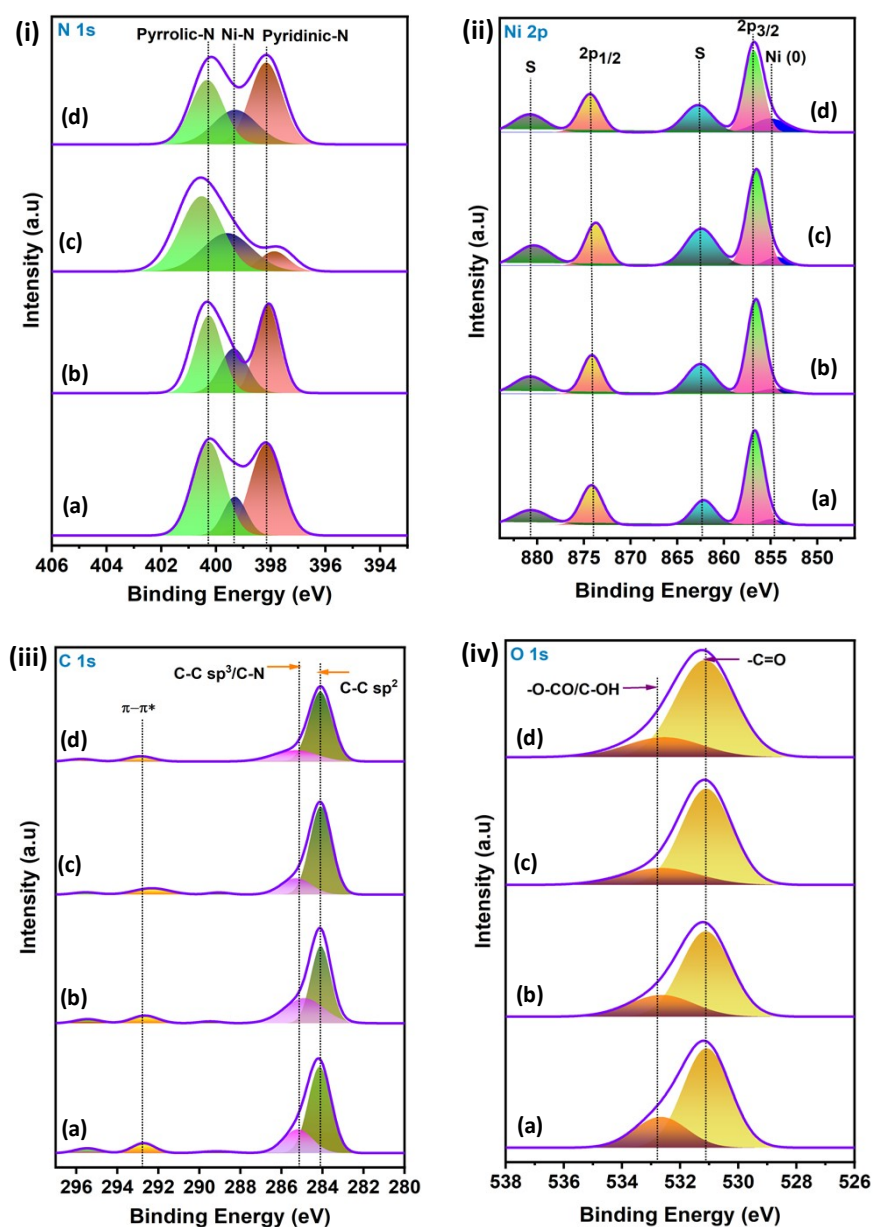


Figure S2: XPS analysis of Ni-NPs@NBC-600 (a), Ni-NPs@NBC-700 (b) Ni-NPs@NBC-800 (c) and spent Ni-NPs@NBC-700 (d) catalysts. (i) N 1s (ii) Ni 2p (iii) C 1s and (iv) O 1s.

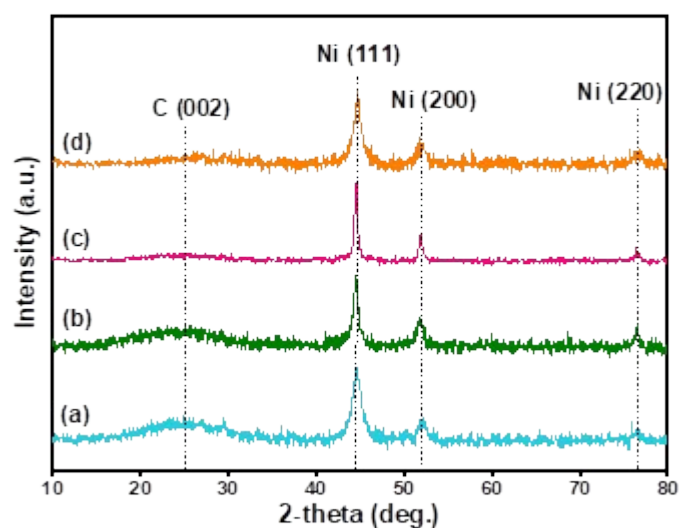


Figure S3: Powder XRD pattern of (a) Ni-NPs@NBC-600, (b) Ni-NPs@NBC-700, (c) Ni-NPs@NBC-800, and (d) spent Ni-NPs@NBC-700R catalysts.

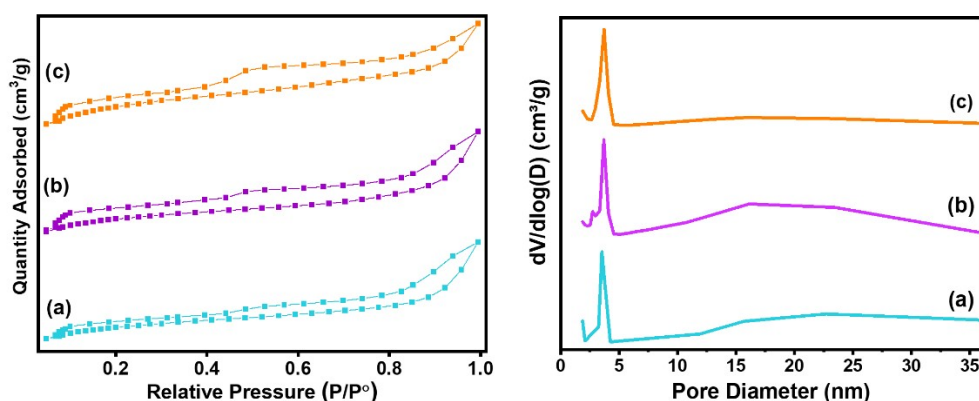


Figure S4: N₂ adsorption-desorption isotherms and pore-size distributions of (a) Ni-NPs@NBC-600, (b) Ni-NPs@NBC-700 and (c) Ni-NPs@NBC-800 catalysts.

Table S3: Surface properties of Ni-NPs@NBC-600, Ni-NPs@NBC-700, Ni-NPs@NBC-800, and spent Ni-NPs@NBC-700R catalysts.

Entry	Catalyst	BET surface area (m ² /g)	Pore Volume (cm ³ /g)
1	Ni-NPs@NBC-600	250	0.092
2	Ni-NPs@NBC-700	285	0.109
3	Ni-NPs@NBC-800	270	0.098
4	Ni-NPs@NBC-700R (spent)	125	0.042

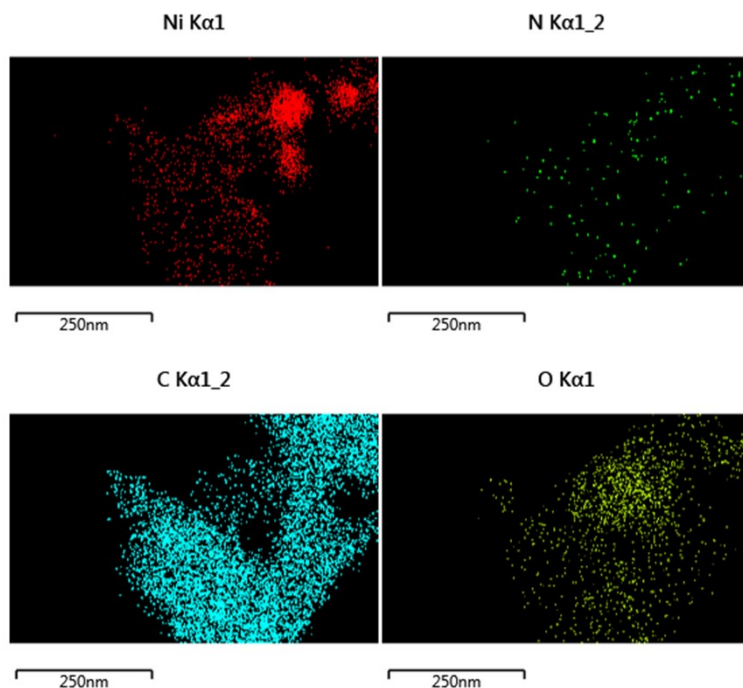


Figure S5: Elemental EDX mapping of Ni-NPs@NBC-700

Table S4: CO₂-TPD measurements of Ni-NPs@NBC-600, Ni-NPs@NBC-700 and Ni-NPs@NBC-800 catalysts.

Entry	Catalyst	Amount of basicity (mmol/g.cat)
1	Ni-NPs@NBC-600	0.415
2	Ni-NPs@NBC-700	0.525
3	Ni-NPs@NBC-800	0.320

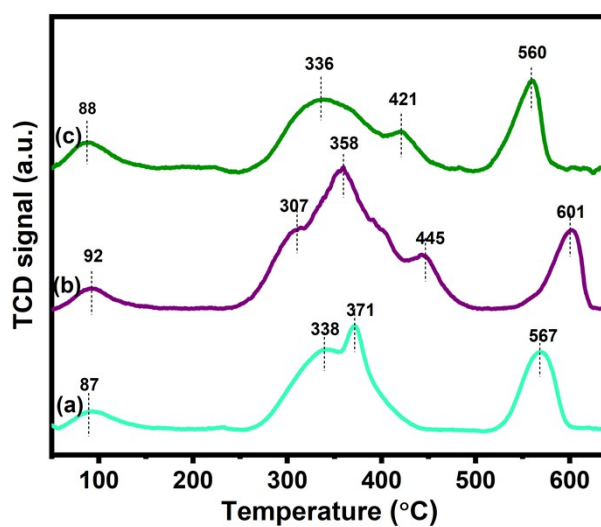


Figure S6. CO₂-TPD profiles of (a) Ni-NPs@NBC-600, (b) Ni-NPs@NBC-700, and (c) Ni-NPs@NBC-800 catalysts

The magnetic behaviour of active Ni-NPs@NBC-700 was measured at 5 K, 100 K, and 300 K with the saturation magnetization (M_s in emu g^{-1}) values 8.6, 7.8, and 7.2, respectively (**Figure S7**). These properties allow facile magnetic separation and fast recovery from the reaction mixture.

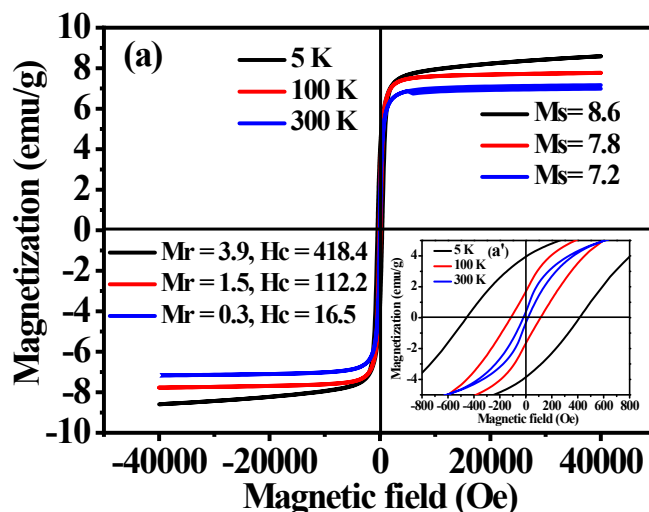
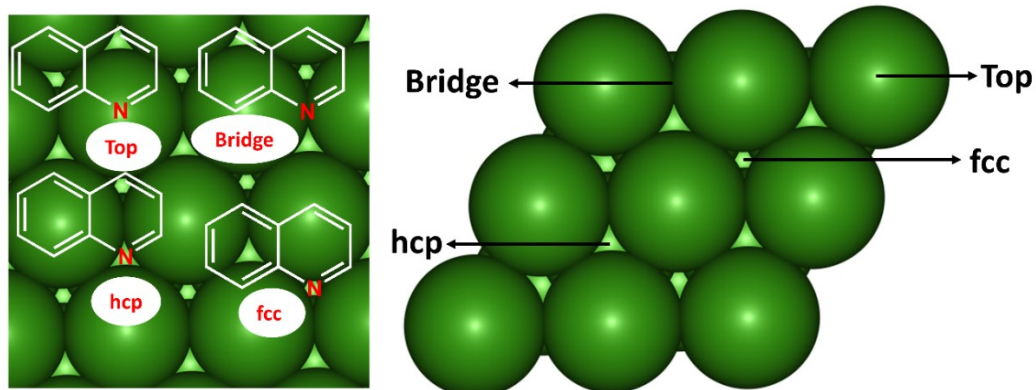


Figure S7: Magnetization curve for the Ni-NPs@NBC-700 catalyst at different temperatures

3. DFT calculation

(a)



(b).

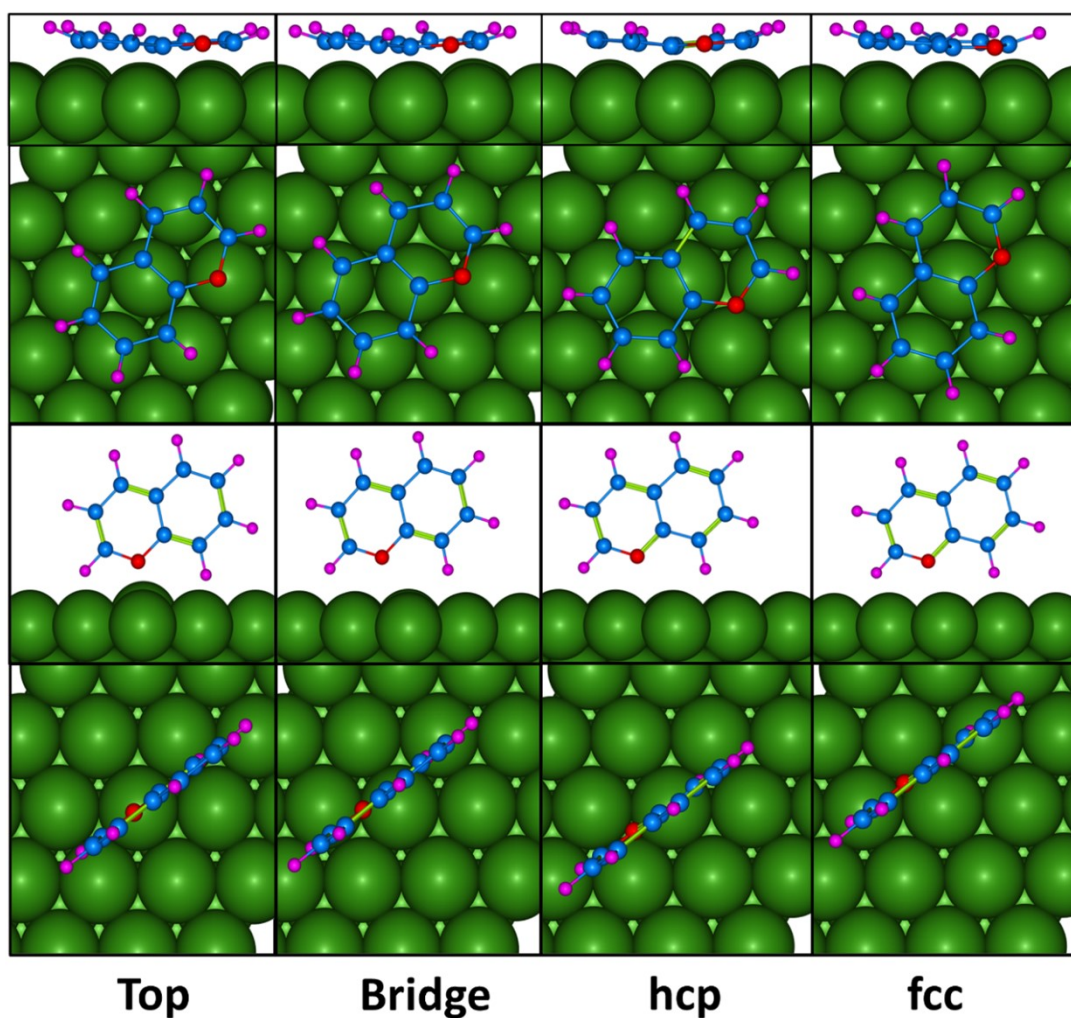
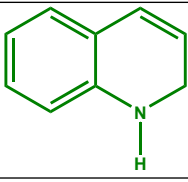
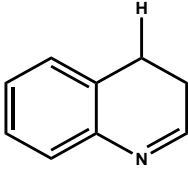
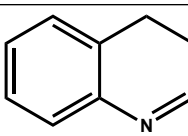
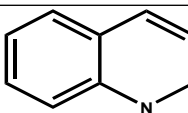
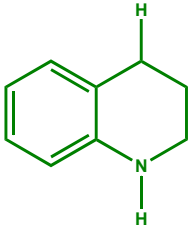
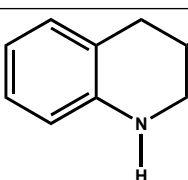
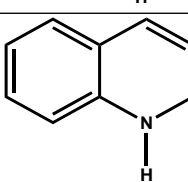


Figure S8. (a). Top view of Ni(111) surface showing the different possible sites. (b). Top view and side view of optimized structures of parallel (top panel) and vertical (bottom panel) adsorption of quinoline on Ni(111) surface.

Table S5. Relative energy of all possible modes of adsorption of Quinoline on Ni(111) surface.

Mode of adsorption	Relative energy (eV)
Parallel Top	0.24
Parallel Bridge	0.00
Parallel hcp	0.21
Parallel fcc	0.07
Vertical Top	1.82
Vertical Bridge	2.35
Vertical hcp	2.37
Vertical fcc	2.37

Table S6. Relative energy of the isomeric products obtained for each reaction intermediate, structure shown in green represent the most stable isomers.

System	Structure	Energy (eV)
C_9H_8N		0.00
		0.45
		0.33
		0.61
C_9H_9N		0.00
		0.01
		0.01

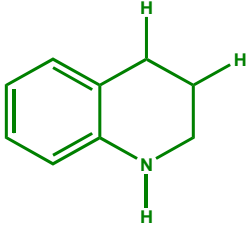
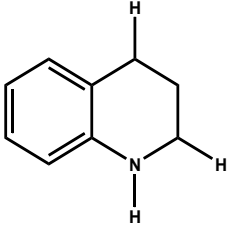
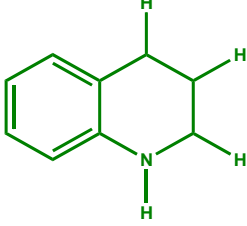
C ₉ H ₁₀ N		0.00
		0.11
C ₉ H ₁₁ N		0.00

Table S7. Distance between most stable adsorbate and the Ni(111) surface.

Adsorbate	Surface-adsorbate distance (Å)
Quinoline	2.16
1-HQ	2.25
1,4-DHQ	2.34
1,3,4-THQ	2.49
1,2,3,4-THQ	2.69

Table S8. Calculated reaction free energy and activation barrier for each elementary step associated with the hydrogenation reaction.

Reaction	Free energy (eV)	Activation barrier (eV)
Q+H → 1-HQ	0.26	0.75
1-HQ+H → 1,4-DHQ	0.61	0.71
1,4-DHQ+H → 1,3,4-THQ	0.30	0.52
1,3,4-THQ+H → 1,2,3,4-THQ	0.11	0.51

Table S9: Comparison of catalyst in this work and other previous state-of-the-art Ni-catalytic systems for the hydrogenation of heteroarenes and arenes.

Entry	Catalyst	Reaction conditions	Scope and limitations	Reference
1	NiNPs@BNC-700	120 °C, 30 bar, 24 h	Applicable for the hydrogenation of both arenes and heteroarenes including hydrogenation of quinolines, quinoxalines, pyridines, pyrrole, indoles, furan and benzofurans. (>40 examples, up to 99% yield). Synthesis of pharmaceutical intermediates is demonstrated. Catalyst is recycled and reused up to 5 cycles	This work
2	Ni/Phen@SiO ₂ -800	130-140 °C, 30-40 bar, 24 h	Applied for the hydrogenation of heteroarenes, (pyridines and quinolines, 18 examples, up to 99% yields). Not used for the hydrogenation of arenes. Catalyst was recycled and reused up to 5 times	ACS Appl. Nano Mater. 2022, 5, 4, 5625–5630 (ref 52)
3	Ni-CeOx/CN-550	120 °C, 20 bar, 14-36 h	Applicable for the hydrogenation of heteroarenes, (quinolines and quinoxalines, 20 examples, up to 99% yields). Not used for the hydrogenation of arenes. Catalyst was recycled and reused up to 5 cycles	Molecular Catalysis, 2023, 540, 113052 (ref 74)
4	Ni-phen@SiO ₂ -1000	120 °C, 50 bar, 20 h	Applicable for the hydrogenation of heteroarenes (quinolines, 5 examples, up to 98% yields). Not used for the hydrogenation of arenes	Sci. Adv., 2018, 4, eaat0761(ref 75)

5	Ni@C-400	120 °C, 20 bar, 2 h	Applied for the hydrogenation of phenol. Note used for the hydrogenation of other arenes and heterocycles	React. Chem. Eng., 2022,7, 170-180 (ref. 79)
6	Ni/CSC	200 °C, 20 bar, 4 h	Applied for the hydrogenation of nitrobenzene to cyclohexylamine. Not applied for the hydrogenation of other aromatic and heteroaromatic compounds	Sci. Rep. 2017, 7, 2676 (ref. 85)
7	Ni/NiCaAlOx	110 °C, 20 bar, 1.5 h	Applied for the hydrogenation of phenol to cyclohexanol. Note used for the hydrogenation of other arenes and heterocycles	Appl. Clay Sci. 2021, 203, 106003 (ref 77)

Heterogeneous Ni-based catalysts are known for the hydrogenation of quinolines, pyridines and indoles. In addition, also for the hydrogenation of simple arenes such as benzene and phenol. However, to the best of our knowledge, there is no Ni-based catalyst reported for the hydrogenation of both arenes and heteroarenes with broad substrate scope including functionalized and structurally diverse ones. Noteworthy our Ni-catalytic system is applied for the hydrogenation of different kinds of heterocycles including quinolines, quinoxalines, pyridines, pyrrole, indoles, furan and benzofurans as well as for the diverse arenes including pharmaceutical intermediates.

Leaching test/heterogeneity test of NiNPs@BNC-700 catalyst: To test the leaching of the catalyst, ICP-OES and hot filtration test were conducted. ICP-OES analysis for the spent NiNPs@NBC-700 catalyst did not show any significant change in amount of the nickel after the recyclability of the catalyst and no amount of nickel for the filtrate after 6 h in the first cycle of reaction. Furthermore, as shown in figure S9, hot filtrate showed negligible yield of 2 under the standard reaction conditions.

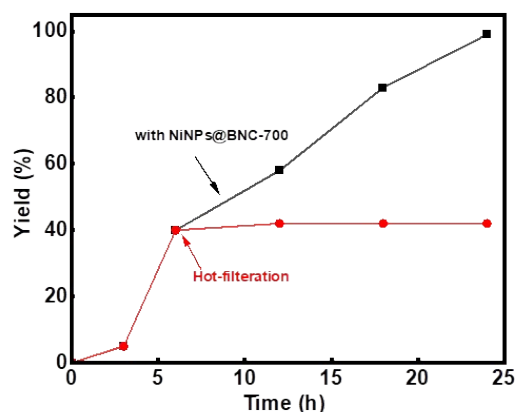


Figure S9: Hot-filtration experiment under standard conditions

Table S9. Effect of other biomass derived Ni-catalysts

Entry	Catalyst	Conversion of 1 (%)	Yield of 2 (%)
1	Ni-NPS@NBC-700	>99	99
2	Ni/Lignin-700	7	3
3	Ni/Cellulose-700	74	72

Reaction Conditions: 0.5 mmol quinoline, 50 mg catalyst, 30 bar H₂, 2 mL isopropanol, 120 °C, and 24 h

4. General procedure for the synthesis of pine needle derived Ni-catalysts

In 100 mL round bottom flask, nickel (II) nitrate hexahydrate (1.23 mg) was dissolved in 20 mL ethanol solvent. Then, dried pine needle (4.75 g) was added in the solution and continuously stirred for 6 h at 50 °C. Next, the solvent was evaporated from the solution mixture, and the obtained solid was kept in an oven at 100 °C for overnight. Finally the dried solid material was crushed to a fine powder and pyrolyzed at various temperatures (500-800 °C) for 3 h in the presence of nitrogen atmosphere to obtain nickel materials (Ni-NPs@NBC-T).

5. General procedure for the hydrogenation of arenes and heteroarenes

Ni-NPs@NBC-700 (50 mg), starting material (0.5 mmol), and isopropanol (2-4 mL) were added to a 25 mL stainless steel autoclave, and it was sealed. Initially, the autoclave was carefully purged with 30 bar hydrogen gas to remove air and then pressurized with hydrogen pressure (30-50 bar). The reaction mixture was allowed to stir at 120-130 °C in an oil bath for 24 h. After completion of the reaction, the autoclave was allowed to cool at room temperature. Then, the remaining hydrogen was carefully discharged. The solid Ni-NPs@NBC-700 nanocatalyst was separated by simple filtration through filter paper. After evaporating the

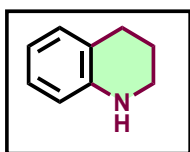
solvent in a rotary evaporator, the obtained crude product was purified by column chromatography (hexane/EtOAc) to achieve the pure product, which was further submitted for analysis by nuclear magnetic resonance (NMR) and gas chromatography-mass spectrometry (GC-MS).

6. General procedure for the recyclability studies

The reaction was performed according to the general procedure for hydrogenation of hetero(arenes). Typically, after completing the reaction, the solid Ni-NPs@NBC-700 nanocatalyst was separated by magnetic separation and through simple filtration over filter paper. The obtained solid catalyst was washed with distilled water and ethanol, then dried in a vacuum oven at 90 °C overnight and used for the next run without any reactivation.

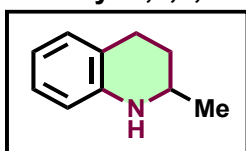
7. Spectral data of products

1,2,3,4-Tetrahydroquinoline



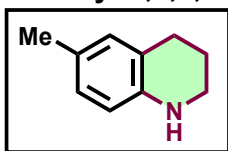
¹H NMR (600 MHz, CDCl₃) δ 7.02 – 6.88 (m, 2H), 6.58 (t, 1H), 6.43 (d, 1H), 3.76 (s, 1H), 3.36 – 3.19 (t, 2H), 2.75 (t, 2H), 1.90 (q, 2H). **¹³C NMR (151 MHz, CDCl₃)** δ 144.89 (s), 129.60 (s), 126.81 (s), 121.49 (s), 116.99 (s), 114.27 (s), 42.06 (s), 27.08 (s), 22.26 (s).

2-Methyl-1,2,3,4-tetrahydroquinoline



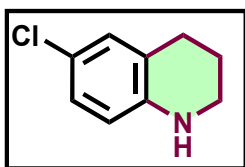
¹H NMR (500 MHz, CDCl₃) δ 7.09 – 6.94 (m, 2H), 6.73 – 6.60 (m, 1H), 6.56 – 6.44 (m, 1H), 4.08 – 3.55 (m, 1H), 3.51 – 3.37 (m, 1H), 2.96 – 2.70 (m, 2H), 1.97 (m, 1H), 1.71 – 1.56 (m, 1H), 1.24 (m, 3H). **¹³C NMR (126 MHz, CDCl₃)** δ 144.92 (s), 129.39 (s), 126.82 (s), 121.22 (s), 117.11 (s), 114.15 (s), 47.29 (s), 30.28 (s), 26.72 (s), 22.73 (s).

6-Methyl-1,2,3,4-tetrahydroquinoline



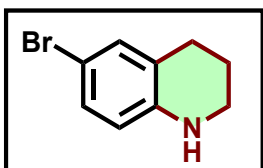
¹H NMR (500 MHz, CDCl₃) δ 6.79 (m, 2H), 6.44 – 6.37 (m, 1H), 3.32 – 3.22 (m, 2H), 2.74 (t, 2H), 2.21 (s, 3H), 2.00 – 1.88 (m, 2H). **¹³C NMR (126 MHz, CDCl₃)** δ 142.50 (s), 130.14 (s), 127.32 (s), 126.32 (s), 121.67 (s), 114.53 (s), 42.27 (s), 27.00 (s), 22.54 (s), 20.46 (s).

6-Chloro-1,2,3,4-tetrahydroquinoline



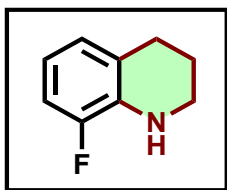
^1H NMR (400 MHz, CDCl_3) δ 6.92 – 6.75 (m, 2H), 6.39 – 6.30 (m, 1H), 3.74 (s, 1H), 3.24 – 3.17 (m, 2H), 2.65 (t, 2H), 1.89 – 1.78 (m, 2H). **^{13}C NMR (101 MHz, CDCl_3)** δ 142.82, 129.08, 126.56, 123.20, 121.63, 115.42, 41.87, 26.81, 21.67.

6-Bromo-1,2,3,4-tetrahydroquinoline



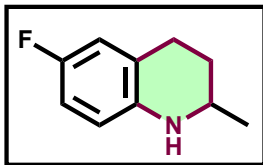
^1H NMR (600 MHz, CDCl_3) δ 7.06 – 7.04 (m, 1H), 7.02 (dd, J = 8.4, 2.3 Hz, 1H), 6.33 (d, J = 8.4 Hz, 1H), 3.29 – 3.26 (m, 2H), 2.72 (t, J = 6.4 Hz, 2H), 1.93 – 1.88 (m, 2H). **^{13}C NMR (151 MHz, CDCl_3)** δ 143.74, 131.88, 129.36, 123.40, 115.53, 108.20, 41.80, 26.83, 21.68.

8-Fluoro-1,2,3,4-tetrahydroquinoline



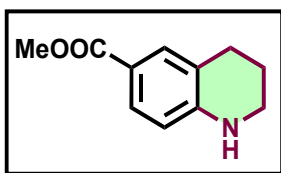
^1H NMR (600 MHz, CDCl_3) δ 6.68 (ddd, J = 9.1, 6.1, 3.0 Hz, 1H), 6.41 (dd, J = 9.5, 4.9 Hz, 1H), 3.28 – 3.25 (m, 1H), 2.74 (t, J = 6.5 Hz, 1H), 1.92 (dt, J = 8.8, 6.4 Hz, 1H). **^{13}C NMR (151 MHz, CDCl_3)** δ 155.5 (d, $J_{\text{C-F}}$ = 232.5 Hz), 140.9, 122.8 (d, $J_{\text{C-F}}$ = 7.5 Hz), 115.6 (d, $J_{\text{C-F}}$ = 22.5 Hz), 114.9 (d, $J_{\text{C-F}}$ = 7.5 Hz), 113.2 (d, $J_{\text{C-F}}$ = 22.5 Hz), 42.09, 27.02, 21.9.

6-Fluoro-2-methyl-1,2,3,4-tetrahydroquinoline



^1H NMR (500 MHz, CDCl_3) δ 6.59 (m, 2H), 6.36 – 6.27 (m, 5H), 3.28 (m, 2H), 2.80 – 2.56 (m, 2H), 1.83 (m, 1H), 1.56 – 1.38 (m, 1H), 1.14 (dd, 3H). **^{13}C NMR (126 MHz, CDCl_3)** δ 156.48 (s), 154.61 (s), 140.95 (s), 122.55 (s), 115.50 (s), 115.33 (s), 114.80 (s), 113.27 (s), 113.09 (s), 47.35 (s), 29.89 (s), 26.73 (s), 22.49 (s). **^{19}F NMR (376 MHz, CDCl_3)** δ -128.26.

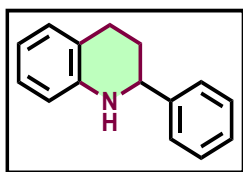
Methyl 1,2,3,4-tetrahydroquinoline-6-carboxylate



^1H NMR (600 MHz, CDCl_3) δ 7.64 – 7.61 (m, 2H), 6.39 – 6.33 (m, 1H), 4.45 (s, 1H), 3.82 (s, 3H), 3.32 – 3.29 (m, 2H), 2.73 (t, J = 6.3 Hz, 2H), 1.92 – 1.86 (m, 2H).

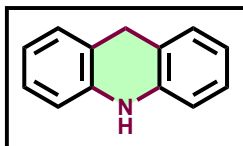
^{13}C NMR (151 MHz, CDCl_3) δ 167.62, 148.93, 131.28, 129.13, 119.85, 117.20, 115.20, 112.63, 51.44, 41.69, 26.94, 21.39.

2-Phenyl-1,2,3,4-tetrahydroquinoline



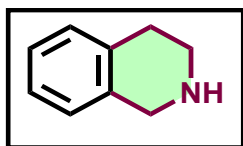
^1H NMR (500 MHz, CDCl_3) δ 7.38 (m, 5H), 7.05 (t, 2H), 6.70 (t, 1H), 6.57 (d, 1H), 4.47 (dd, 1H), 4.09 (s, 1H), 2.96 (m, 1H), 2.78 (m, 1H), 2.23 – 2.11 (m, 1H), 2.11 – 1.96 (m, 1H). **^{13}C NMR (126 MHz, CDCl_3)** δ 144.80 (s), 129.36 (s), 128.63 (s), 127.50 (s), 126.96 (s), 126.61 (s), 120.95 (s), 117.23 (s), 114.07 (s), 56.31 (s), 31.03 (s), 26.43 (s).

4a,9,9a,10-Tetrahydroacridine



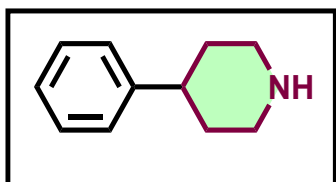
^1H NMR (500 MHz, CDCl_3) δ 7.08 (m, 4H), 6.85 (m, 2H), 6.66 (m, 2H), 5.94 (s, 1H), 4.05 (s, 2H). **^{13}C NMR (126 MHz, CDCl_3)** δ 140.13 (s), 128.63 (s), 127.02 (s), 120.65 (s), 120.05 (s), 113.45 (s), 31.40 (s).

1,2,3,4-Tetrahydroisoquinoline



^1H NMR (500 MHz, CDCl_3) δ 7.17 – 7.02 (m, 2H), 7.02 – 6.94 (m, 2H), 4.02 – 3.93 (m, 2H), 3.15 – 3.07 (m, 2H), 2.83 – 2.74 (m, 2H), 2.64 (s, 1H). **^{13}C NMR (151 MHz, CDCl_3)** δ 135.78, 134.75, 129.34, 126.26, 126.07, 125.77, 48.24, 43.85, 29.14.

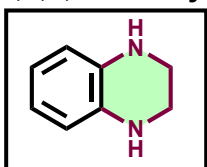
4-Phenylpiperidine



^1H NMR (600 MHz, CDCl_3) δ 7.30 (t, J = 7.6 Hz, 2H), 7.20 (ddd, J = 8.5, 6.5, 4.3 Hz, 3H), 3.76 (s, 1H), 3.24 (d, J = 12.2 Hz, 2H), 2.80 – 2.72 (m, 2H), 2.63 (tt, J = 12.1, 3.6 Hz, 1H), 1.85 (d, J = 13.0 Hz, 2H), 1.72 (qd, J = 12.7, 3.8 Hz, 2H).

^{13}C NMR (151 MHz, CDCl_3) δ 146.3, 128.4, 126.8, 126.2, 46.7, 42.7, 33.8

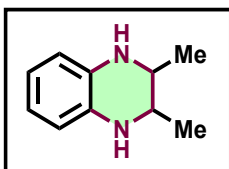
1,2,3,4-Tetrahydroquinoxaline



^1H NMR (500 MHz, CDCl_3) δ 6.66 – 6.54 (m, 2H), 6.54 – 6.44 (m, 2H), 3.61 – 3.31 (m, 6H).

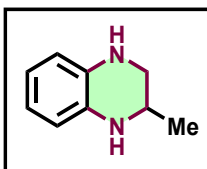
^{13}C NMR (126 MHz, CDCl_3) δ 133.57 (s), 118.87 (s), 114.82 (s), 41.37 (s).

2,3-Dimethyl-1,2,3,4-tetrahydroquinoxaline



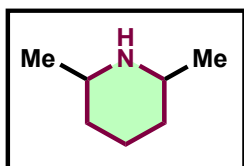
^1H NMR (500 MHz, CDCl_3) δ 6.58 (dt, 2H), 6.54 – 6.44 (m, 2H), 3.56 – 3.41 (m, 2H), 3.42 – 2.66 (m, 2H), 1.13 (d, 6H). **^{13}C NMR (126 MHz, CDCl_3)** δ 132.51 (s), 118.68 (s), 114.54 (s), 49.03 (s), 17.17 (s).

2-Methyl-1,2,3,4-tetrahydroquinoxaline



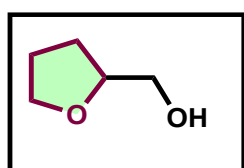
^1H NMR (500 MHz, CDCl_3) δ 6.67 – 6.31 (m, 4H), 5.90 – 5.85 (m, 1H), 3.55 – 3.40 (m, 2H), 3.25 (m, 1H), 3.05 – 2.91 (m, 1H), 1.24 – 1.15 (m, 1H), 1.12 (d, 3H). **^{13}C NMR (126 MHz, CDCl_3)** δ 133.41 (s), 133.04 (s), 118.86 (s), 114.61 (s), 48.19 (s), 45.74 (s), 19.85 (s).

2,6-Dimethylpiperidine



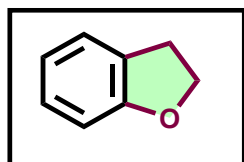
^1H NMR (500 MHz, CDCl_3) δ 4.18 – 4.10 (m, 1H), 3.98 – 3.89 (m, 1H), 2.15 – 1.87 (m, 2H), 1.57 – 1.41 (m, 2H), 1.23 (dd, 6H). **^{13}C NMR (126 MHz, CDCl_3)** δ 75.26 (s), 74.41 (s), 34.17 (s), 33.02 (s), 21.39 (s).

(Tetrahydrofuran-2-yl)methanol



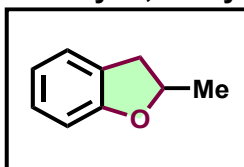
^1H NMR (400 MHz, CDCl_3) δ 3.98 – 3.86 (m, 1H), 3.84 – 3.74 (m, 1H), 3.74 – 3.64 (m, 1H), 3.55 (dd, 1H), 3.42 (dd, 1H), 3.26 (s, 1H), 1.91 – 1.72 (m, 3H), 1.65 – 1.47 (m, 1H). **^{13}C NMR (101 MHz, CDCl_3)** δ 79.62, 68.15, 64.71, 27.14, 25.86.

2,3-Dihydrobenzofuran



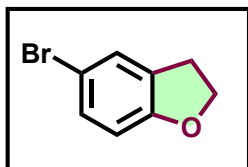
^1H NMR (500 MHz, CDCl_3) δ 7.26 – 7.10 (m, 2H), 6.86 (m, 2H), 4.57 (t, 2H), 3.22 (t, 2H). **^{13}C NMR (126 MHz, CDCl_3)** δ 160.16 (s), 128.02 (s), 126.97 (s), 124.99 (s), 120.42 (s), 109.45 (s), 71.08 (s), 29.85 (s).

2-Methyl-2,3-dihydrobenzofuran



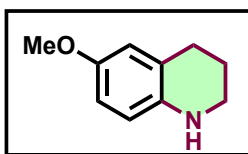
^1H NMR (600 MHz, CDCl_3) δ 7.20 (dd, J = 7.3, 0.9 Hz, 1H), 7.17 – 7.13 (m, 1H), 6.87 (td, J = 7.4, 0.9 Hz, 1H), 6.83 – 6.80 (m, 1H), 4.99 – 4.91 (m, 1H), 3.34 (dd, J = 15.3, 8.8 Hz, 1H), 2.85 (dd, J = 15.3, 7.7 Hz, 1H), 1.51 (d, J = 6.3 Hz, 3H). **^{13}C NMR (151 MHz, CDCl_3)** δ 159.5, 128.0, 127.0, 125.0, 120.2, 109.3, 79.5, 37.1, 21.8

5-Bromo-2,3-dihydrobenzofuran



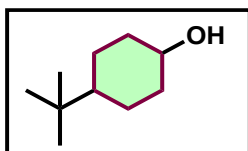
¹H NMR (600 MHz, CDCl₃) δ 7.28 – 7.26 (m, 1H), 7.20 – 7.17 (m, 1H), 6.65 (d, J = 8.5 Hz, 1H), 4.56 (t, J = 8.7 Hz, 2H), 3.18 (t, J = 8.7 Hz, 2H). **¹³C NMR (151 MHz, CDCl₃)** δ 159.2, 130.6, 129.5, 127.8, 112.0, 110.8, 71.5, 29.6

6-Methoxy-1,2,3,4-tetrahydroquinoline



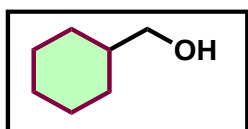
¹H NMR (600 MHz, CDCl₃) δ 6.62 (dd, J = 8.6, 2.9 Hz, 1H), 6.59 (d, J = 2.8 Hz, 1H), 6.47 (d, J = 8.6 Hz, 1H), 3.75 (s, 3H), 3.45 (s, 1H), 3.28 – 3.25 (m, 2H), 2.77 (t, J = 6.5 Hz, 2H), 1.97 – 1.91 (m, 2H). **¹³C NMR (151 MHz, CDCl₃)** δ 151.84, 138.91, 122.92, 115.64, 114.89, 112.92, 55.82, 42.37, 27.21, 22.48.

4-(Tert-butyl)cyclohexanol



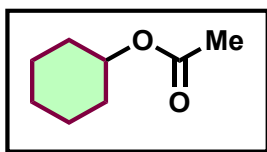
¹H NMR (600 MHz, CDCl₃) δ 4.01 – 3.75 (m, 0.49 cis-CHOH), 3.44 (m, 0.49 trans-CHOH), 2.85 (s, 1H), 2.42 – 0.92 (m, 13H), 0.91 – 0.72 (m, 4H). **¹³C NMR (151 MHz, CDCl₃)** δ 66.0, 48.2, 33.5, 32.7, 27.6, 21.0.

Cyclohexylmethanol



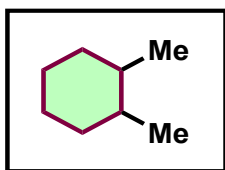
¹H NMR (500 MHz, CDCl₃) δ 3.39 (dd, 2H), 2.27 (d, 1H), 1.78 – 1.54 (m, 5H), 1.48 – 1.34 (m, 1H), 1.30 – 1.00 (m, 3H), 0.97 – 0.75 (m, 2H). **¹³C NMR (126 MHz, CDCl₃)** δ 68.64 (s), 40.49 (s), 29.65 (s), 26.65 (s), 25.90 (s).

Cyclohexyl acetate



^1H NMR (400 MHz, CDCl_3) δ 4.70 (m, 1H), 1.99 (s, 3H), 1.87 – 1.74 (m, 2H), 1.74 – 1.63 (m, 2H), 1.57 – 1.46 (m, 1H), 1.43 – 1.28 (m, 4H), 1.28 – 1.15 (m, 1H). **^{13}C NMR (101 MHz, CDCl_3)** δ 170.48, 72.59, 31.61, 25.34, 23.76, 21.35.

1,2-di methylcyclohexane



^1H NMR (400 MHz, CDCl_3) δ 1.77 – 1.49 (m, 1H), 1.49 – 0.96 (m, 2H), 0.89 (t, $J = 13.4$ Hz, 2H). **^{13}C NMR (101 MHz, CDCl_3)** δ 39.17, 35.81, 34.16, 31.24, 26.86, 23.50, 20.27, 15.87.

8. Copies of NMR spectra

